Development of PERL Solar Cell

Yang Li[1, *, †], Yangming Zhang[2, *, †]

[1]School of EESE, University of Birmingham, United Kingdom, B15 2TT

[2]Room 246, north courtyard, Wangjiang campus, Sichuan University, Chengdu, Sichuan Province, China, 610044

*Corresponding author: yxl1108@student.bham.ac.uk

[†]These authors contributed equally.

Keywords: Development of silicon solar cells, Manufacturing technology of battery structure, Commercialization of battery products.

Abstract: This paper reviews the development of the passivated emitter, rear locally diffused (PERL) silicon solar cell. The main focus of this text is on the fabrication technologies available to process such cell structure. When PERL solar cell was first introduced, it achieved an efficiency record of 24% in a laboratory setting. However, it had very limited commercial usage due to its complex fabrication process. Nowadays, companies such as Suntech Power has commercialised products based on PERL cells. Thus, reviewing all the fabrication technics that can be implemented to manufacture PERL solar cells might enable us to transform certain advanced laboratory fabrication technics to be suitable for commercial usage.

1. Introduction

Ever since the first practical solar cell was produced in the Bell laboratories [1], great potential has been demonstrated from these devices that are capable of harvesting energy from the sun. With the escalating situation of climate change and the world leaders promising to achieve “net zero” by the middle of this century [2], more efficient solutions for renewable energy generation are being looked at closely, such as solar cells which have higher conversion efficiencies. In this paper, the history of development and the fabrication process of the passivated emitter, rear locally-diffused (PERL) cells will be discussed comprehensively. Section 1 reviews the timeline of the PERL cell development from its invention in 1990 [3]. Its inception was based on the earlier passivated emitter and rear cells (PERC). The heavily doped p+ regions at the rear side of the cell is a distinguishing feature of the PERL solar cell. Hence, the boron diffusion process used to form those p+ regions will be discussed in detail. In 1993, further improvements were made by adding the “alneal” process which made double layer antireflective coating possible [4, 5]. Section 2 reviews technics such as laser chemical processing (LCP) that are used in the manufacturing process of solar cells [6, 7, 8, 9]. In section 3, an attempt to explore technics that can improve the efficiency of the PERL cells will be made.

2. History

2.1 Invention (1990 – 1992)

(1) From PERC to PERL Cells (1990 - 1992). The PERL cell structure was first introduced in 1990 in the Solar Photovoltaic Laboratory at the New South Wales University as an improvement over the earlier passivated emitter and rear cells (PERC) [3]. The PERL cell had a good energy conversion efficiency of 23.1% in 1990.

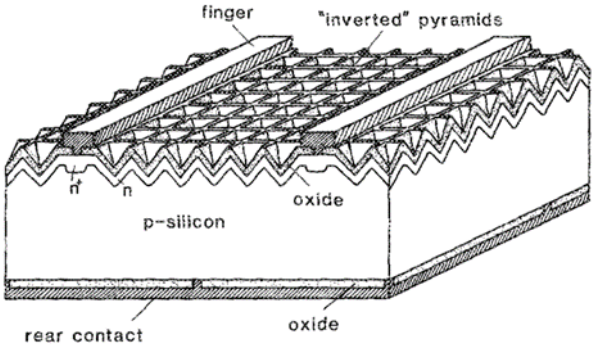

Figure 1. Schematic Diagram of a PERC Cell. Reprinted from [10]

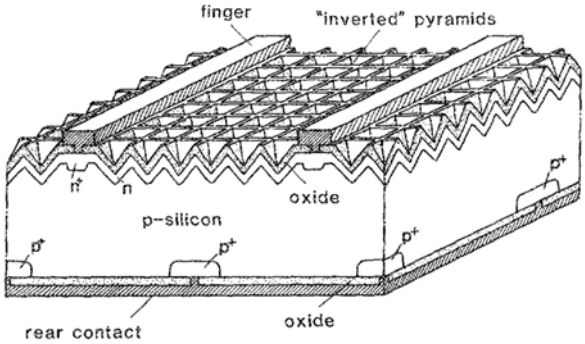

Figure 2. Schematic Diagram of a PERL Cell. Reprinted from [3]

The difference between the PERC cells and PERL cells can be spotted by comparing Figures 1 and 2 above [3, 10]. Unlike the PERC cells, the p-silicon substrate at the rear contact points of the PERL cells is heavily doped with boron, which reduces the minority carrier concentrations at those points. Hence, the effective recombination rate at the rear is suppressed. It is not shown in the figures above, but the opening gaps of the rear oxide layer in the PERL cell may be reduced to achieve lower cell lateral series resistance.

(2) Heavy Boron Diffusion Under the Rear Metal Contact Area [4]. A boron diffusion technique with solid or spin-on sources was experimented with to form the heavily doped p+ region shown at the bottom side of Figure 2. The results were non-ideal as the surface recombination rate increased and the performance of the cells decreased. Aluminium was also experimented with as a diffusion source. However, the diffusion process of aluminium causes significant contamination. Hence, the boron tribromide liquid source was used as the diffusion source. This is a common diffusion source in the semiconductor industry. However, modifications to the diffusion process need to be made in order to achieve high minority carrier lifetimes for high-efficiency solar cells.

For BBr3 diffusion, it was found that the early normal boron diffusion experiments, which diffused BBr3 directly to the silicon, generated defects at the silicon surface. These defects, including the stacking faults, which can even spread through the silicon, drastically reduced the effective minority carrier lifetime in the substrate. The boron rich layer (BRL) generated in the process was believed to be responsible for the defect generation.

So, a thin oxide layer was grown before the boron source deposition, and the boron was diffused only through this thin oxide, which could reduce the thickness of the BRL, hence reducing the number of defects. Also, this process would reduce the doping concentration but the diffusion time was prolonged.

The thickness of the pre-grown thin protection oxide is critical for the boron diffusion. If the pre-grown oxide were too thick, it would be difficult to diffuse boron through it due to the low diffusion coefficient of boron in silicon dioxide. If it were too thin, it would not protect the underlying silicon surface from reacting with the boron rich glass. Hence, experiments were conducted to determine what

thickness was the best for this pre-grown oxide. It was found that the optimised thickness for different conditions lay from 50Å to 150Å.

When the oxygen partial pressure is very low, BBr_3 will react with the thin pre-grown oxide to generate B_2O_3. In the case with a reasonably high oxygen component in the gas flow, BBr_3 reacts with the oxygen component instead of the thin oxide layer to generate B_2O_3:

$$4BBr3 + 3O2 => 2B2O3 + 6Br2 \quad (1)$$

The thin oxide can also protect the underlying silicon surface from being etched by Br_2, the by-product of the reaction:

$$Si + 2Br2 \Leftrightarrow SiBr4 \quad (2)$$

After numerous trials at different conditions, the optimal processing sequence for BBr3 diffusion is as follows. There must be 4% - 6% oxygen component in the main nitrogen atmosphere for pre-oxidation and source deposition steps. Adapting to the required diffusion profile and surface passivation, the time for pre-oxidation can range from 5 to 20 minutes and the time for source deposition is from 10 to 40 minutes. The diffusion temperature should be controlled from 900°C to 950°C. As BBr3 gas is toxic, the furnace must be purged with the same gas flow of oxygen and nitrogen to expel the BBr3 before the wafers can be extracted from the furnace.

After the boron source deposition, boron atoms need to be diffused deep and heavily to the rear contact areas. To achieve that, set the temperature of the furnace to between 1000°C to 1100°C for several hours while maintaining the same gas flow as the deposition step.

2.2 Improvements (1992 – 1993)

According to Zhao J et al. [5], some new features were added to the original PERL cell in 1993, resulting in significant improvement in the cell efficiencies up to 24%. A schematic diagram of the new design is shown in Figure 3.

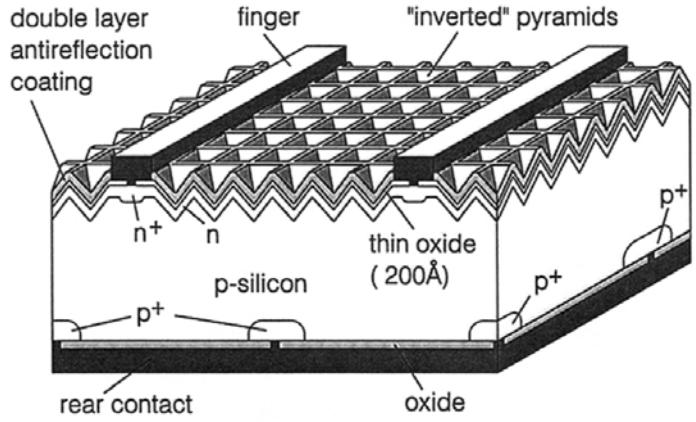

Figure 3. Improved Design of the PERL Cell. Reprinted from [5]

The most distinguishable feature added to the design is the combination of double-layer antireflection (DLAR) coating and the thin oxide layer (200Å). In the previous design, there was only one oxide layer applied to the front surface of the cell, acting as a surface passivation layer and a single layer antireflection (SLAR) coating, as in Figure 2.

(3) Double Layer Antireflection (DLAR) Coating. DLAR was first implemented on PERL cells in 1993 [11]. The oxide layer below the coating must be thinner than 250 Å for the DLAR coating to be effective, but the oxide layer at this thickness cannot provide adequate surface passivation for the cell. Without adequate surface passivation, the performance of the cell would decrease. The solution was found by adding an “alneal” (aluminium anneal) process into the top oxide growing procedure. The details of the “alneal” process will be discussed in detail in section 2.2.2.

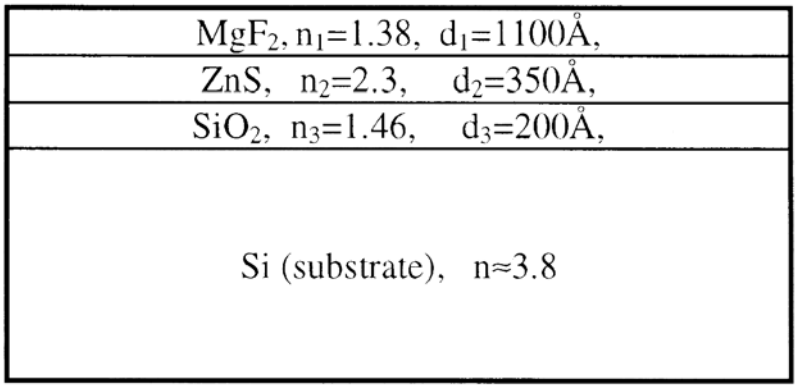

Figure 4. The Surface DLAR Coating Structure for the Standard PERL Cells. Reprinted from [12]

At one time before, the DLAR coatings (MgF2 /ZnS) were settled by the method of vacuum thermal evaporation at the room temperature at UNSW, which caused the coatings' packing density to be relatively low. If the density is relatively low, the voids in the layers are large, and it is easy for the water molecules to fill in these voids when the cells are revealed to the atmosphere. So, these types of films made by the method had the properties dependent upon the humidity. The humidity could influence the dependability and durability of the films. The small portions of films may be got rid of after the coating evaporation straight during the tape peeling tests.

However, research showed that the packing density and the whole quality of the DLAR coatings could be dramatically improved if we heat the substrate to a high temperature when the films were settled. At the higher substrate temperature, the molecules of the coating materials have stronger surface mobility. So, the density could be increased through the high mobility of the molecules. Such films with high dense would have higher resistance not only to the humidity but also to other chemicals too.

Hence, using vacuum thermal evaporation [12], MgF2/ZnS DLAR coatings were settled on the surface of SiO2, as shown in Figure 4. The evaporation was carried out at the vacuum pressure of around 2 × 10-6 Torr. To enhance the Homogeneity of the films, a special device called the planetary motion system was applied to deposit the ZnS and MgF2 sources. Lamps situated in the vacuum chamber were used to heat the substrates. The temperature of the substrate was controlled and adjusted by a temperature controller and supervised by a thermocouple. Two tungsten boats were used to place the ZnS and MgF2 sources. The deposition rates were set for ZnS with 3 Å/s and for MgF2 with 10 Å/s. An Inficon crystal detector was used to monitor the deposition rates. To adjust the deposition rates, the current through the source boats can be changed. An ellipsometer was used to measure the thicknesses of each coating layer and the silicon dioxide that is below them.

Compared to the silicon dioxide-coated PERL cells with the single-layer which was used earlier, the DLAR coated cell has a lower weighted reflection (over 2.5%) [5]. Their performances in the medium and long wavelengths are similar. However, because of the wider external response, the cell with double layer coated has a significantly enhanced external response over the range from 0.8 to 1.1-micron wavelength. Below 0.4-micron wavelength, the absorption in the ZnS layer decreased the cell response. Furthermore, using disparate materials could possibly decrease this loss.

(4) Alneal (Aluminium Anneal) [5] As mentioned before, the thickness of the oxide layer under the DLAR coating is limited to 250Å. To achieve adequate surface passivation with this thickness, an aluminium layer *needs* to be evaporated onto the front surface of the cell. This process is called the aluminium anneal, hence "alneal".

An attempt was also made to etch an appropriate amount of the oxide layer off. Then, the thickness of the oxide would be able to allow DLAR coating to be applied. However, as the etching process could not achieve the required uniformity, this approach was abandoned.

In the "alneal" process, the cell front surface is evaporated with aluminium. Then, the cells are annealed in forming gas at the temperature around 370°C for about 30 min, covered with the

evaporated aluminium. Using phosphoric acid, the aluminium layer is etched off. It is worth noting that the aluminium around the cell periphery should be kept under photoresist as an aperture mask to make the cell area accurately defined. It is very important to have these “alnealed” areas at the peripheral of the top surface since these not doped areas can have a much higher surface recombination rate without “alnealing”. As aluminium is used as the rear contact metal, this “alneal” process is already included in the processing of the rear surface of the cell. The difference between the “alneal” process of the surfaces is that the aluminium layer at the back is not etched off.

Table 1. The Performance of PERL Cells with Different Oxide Thicknesses. The oxide has been grown in a TCA Ambient and Annealed in Forming Gas

Cell ID	Oxide thickness	Jsc (mA/cm2)	Voc (mV)
W4-19-2E	200	36.5	682
Z4-16-2E	600	37.5	697
W4-6-1H	1100	40.7	703

Table 1 above shows the performance of cells processed without the “alnealing” process. The highest open-circuit voltage ever achieved is 703 mV. By repeating the same fabrication process with added “alneal” process, the highest open-circuit voltage ever achieved is up to 709 mV.

2.3 Improvements (1993 – 1999)

According to Zhao J, Wang A and Green MA [6], high-quality FZ (float zone) substrates had been widely used for high-efficiency silicon solar cells research. After 1995, a brightly etched Wacker FZ wafer was experimented with, weeding out the traditional wafers polished on the double-side mechanically. The led to the efficiency record of 24.4% for a PERL cell on an FZ substrate, which was recorded at the 2nd World PV Conference in Vienna, 1998. According to Zhao J, et al. [7], the PERL cell processing has also been further optimised for high carrier lifetime p-type FZ silicon wafers with 1.0 ohm/cm resistivity and 450 mm thickness, provided by the Wacker, Germany. The optimised substrates improved the current density. A planetary motion vacuum coating system could have contributed to an enhanced quality of the antireflection coatings for these cells, as well as an enhanced uniformity of the coatings. The ZnS/MgF2 films coated with this new technology seem to give less absorption of UV light, which could get 24.7% efficiency under the standard global AM1.5 spectrum (100 mW/cm^2) at 25°C.

3. Methods in Production

According to Kluska S and Granek F [11], an industrially workable front and rear side treatment method can be used to partially open the passivation layer and use laser chemical treatment (LCP) to dope silicon below. The principle and benefits of LCP will be discussed in detail in the following paragraphs. Coupling the laser beam into the liquid jet, LCP can be used to form the local n-type doping or p-type doping so as to compose selective emitter and local back surface field (LBSF) structure for the p-type or the n-type solar cells. The selective emitter for the n-type using LCP has shown good results in the laboratory and in the industry. Optimal PERL solar cell efficiency can be up to η= 20.9%, $\Delta\eta$= 0.3-0.4%abs.

According to Kray D, Fell A et al. [12], the principle of LCP: a hairy liquid jet is created in the nozzle with a window that is transparent at the top. The laser beam is centralised into the jet and lead in the jet via the total internal reflection through this window. Laser evaporation or heating can be used together with physicochemical reactions like the etching process, doping process or deposition process depending on the liquid used. The technology is based on synova®, which is the company’s commercial water jet guided laser.

Because of the creation of SiNx antireflection coating, LCP using carrier liquid containing dopant offers a more convenient and simple process; the damage etching, emitter diffusion and the etching process of phosphosilicate glass are applied together in a single micro-structure phase. So we tested LCP with two phosphoric acids: one H3PO4 and the other H3PO3 recently. We can prove that the

slotting of the silicon wafer can certainly be combined with phosphorus doping, and the shape and structure of the emitter will be strongly affected by the intensity of the laser and the type of carrier liquid. The electrical quality of the LCP transmitter is studied by the sun – VOC measurement, which allows the recording of the series non-resistance IV curve of the solar cell or solar cell precursor. In the space charge region, the filling factor of the curve (called a pseudo filling factor) is a measurement method of shunt resistance and recombination. As shown in Table 1, some typical values are displayed for measuring h3po4-ice using infrared and green Nd: YAG lasers. Since these are equal to or even more than eighty per cent, we could conclude the emitters which have low recombination and non-shunt PN junctions are produced. Therefore, we use this technology and frequency-doubled Nd: YVO4 laser to process solar cells. In Fig. 4, the LBIC (Beam Induced Current) diagram of the solar cell is displayed, which shows the uniform carrier collection in the solar cell, expressing a steady and defect-free LCP diffusion process.

According to Kim T, Lim JK et al. [13] and Cornagliotti e, Uruena a et al. [14], a conversion efficiency of 21% was achieved using the PERL type solar cells with pre-electroplating contacts. The 156mm p-type Czochralski silicon wafer used in industry is used as the substrate. Our battery adopts a single-sided texture, single-sided emitter and a double-layer antireflection coating which includes the silicon nitride by PECVD and the thermal silicon oxide. The back is passivated by the dielectric lamination (Al2O3 – SiOxNy). The rear contact is formed by screen printing and laser ablation opening emitting electrodes made of aluminium. Nickel silver or nickel-copper silver contact points are electroplated on the front by light-induced plating (LIP). This Perl cell process makes it possible to achieve the conversion efficiency of 21.0% on a commercial 156 mm Czochralski silicon wafer. Compared with batteries metallised by silver vermicelli screen printing, nickel-plated copper silver front contacts are expected to significantly save costs.

According to Tous L et al. [15], a new front-end contact is proposed. We use metal nickel and copper with silver as the front contact instead of the traditional silver only contact. Nickel/copper contacts provide not only low resistivity but also provide low contact resistance, especially at a low surface concentration (NS). In addition, due to the self-aligning nature of electroplating, it is limited only through the dielectric opening technology and the resulting opening width. These characteristics make the optimal low ns = 1 × 1019 / cm3 uniform n + profile can be compared with narrow (< 10 μm) Laser openings are used in combination to produce linewidth. After electroplating, it is much lower than 50 μm。 In addition, sintering by silver paste usually requires a sintering temperature from 700 to 850 °C. Nickel/copper contacts are usually sintered in the range from 250 to 450 °C. The lower sintering temperature provides excellent back dielectric / Aluminum reflection in PERL cells because aluminium melting does not occur and allows the use of optional dielectric layers, whose passivation performance decreases with high-temperature treatment.

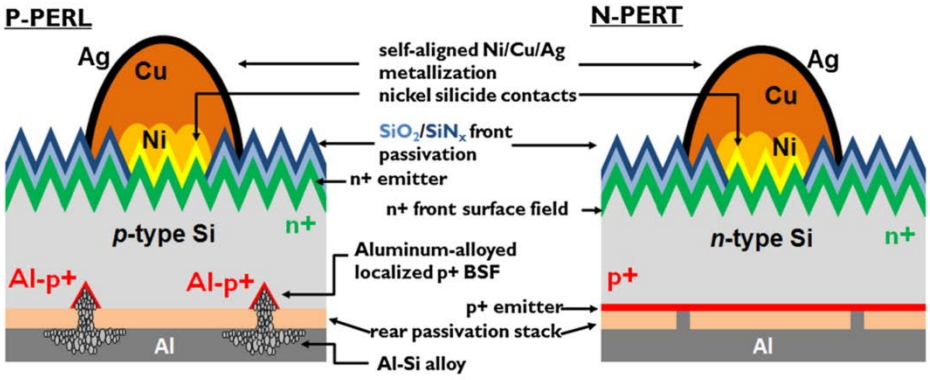

Figure 5. PERL and PERT Large Area Solar Cells with Nickel/Copper/Silver (Ni/Cu/Ag) Plated Front Side Contacts. Reprinted from [15]

4. Conclusion

In 1990, the PERL cell structure was first introduced in the Solar Photovoltaic Laboratory at the University of New South Wales. The newly developed boron diffusion technique with BBr3 liquid source giving low surface damage supplied a method to passivate the rear metal contact areas further. This led to the development of the PERL cell demonstrated an independently confirmed efficiency of 23.3% (AM1.5, 25°C). In 1993, the "alneal" (aluminium anneal) process and double antireflection layers were introduced. Also, the width of the front contacting line was reduced from 2.5 μm to 2 μm with a dotted contact structure to reduce the emitter contact areas. After these improvements, the efficiency had reached 24%. From 1993 to 1999, a sightly etched Wacker FZ wafer was used instead of the double-side mechanically polished wafers. The new efficiency recorded for a PERL silicon cell on an FZ substrate is then 24.4%. Later, the p-type FZ silicon wafers of 1.0 ohm /cm resistivity and 450 mm thickness were used and a recently installed planetary motion vacuum coating system was utilised to get 24.7% efficiency under the standard global AM1.5 spectrum (100 mW/cm2) at 25°C.

In the industrial process, laser chemical processing (LCP) can be used in the doping process and get efficiencies up to 20.9%. And the structure included a single-sided texture, single-sided emitter and a double-layer antireflection coating which consisted of the silicon nitride by PECVD and the thermal silicon oxide. The back can be passivated by the dielectric lamination (Al2O3 – SiOxNy); the rear contact is formed by screen printing and laser ablation opening emitting electrode made by aluminium. Nickel silver or nickel-copper silver contact points are electroplated on the front by light-induced plating (LIP). This PERL cell processing approach makes it possible to achieve the conversion efficiency of 21.0% on a commercial 156 mm Czochralski silicon wafer. And the new front contact with Ag, Ni, and Cu structure can be implemented to get the 20.5% energy conversion efficiencies.

References

[1] Green MA. The Path to 25% Silicon Solar Cell Efficiency: History of Silicon Cell Evolution. Progress in Photovoltaics: Research and Applications. 2009; 17(3): 183-189. Available from: https://onlinelibrary.wiley.com/doi/epdf/10.1002/pip.892 [Accessed 5th November 2021]

[2] Hoegh-Guldberg O, Jacob D, Taylor M, etc. The human imperative of stabilising global climate change at 1.5°C. Science. 2019; 365(6459). Available from: https://www.science.org/doi/10.1126/science.aaw6974 [Accessed 23th November 2021]

[3] Zhao J, Wang A, Green MA. 24% Efficient PERL Structure Silicon Solar Cells. IEEE Conference on Photovoltaic Specialists. 1990; 1: 333-335. Available from: https://ieeexplore.ieee.org/abstract/document/111642 [Accessed 23th November 2021]

[4] Wang A. HIGH EFFICIENCY PERC AND PERL SILICON SOLAR CELLS. 1992. Available from: http://unsworks.unsw.edu.au/fapi/datastream/unsworks:36465/SOURCE01?view=true [Accessed 26th November 2021]

[5] Zhao J, Wang A, Altermatt PP, etc. 24% Efficient perl silicon solar cell: Recent improvements in high efficiency silicon cell research, Solar Energy Materials and Solar Cells. 1996; 41-42: 97-99. Available from: https://doi.org/10.1016/0927-0248(95)00117-4 [Accessed 26th November 2021]

[6] Zhao J, Wang A and Green MA. 24.5% Efficiency silicon PERT cells on MCZ substrates and 24.7% efficiency PERL cells on FZ substrates. Progress in Photovoltaics. 1999; 7(6): 471-474. Available from: https://onlinelibrary.wiley.com/doi/abs/10.1002/(SICI)1099-159X(199911/12)7:6%3C471:AID-PIP298%3E3.0.CO;2-7 [Accessed 23th December 2021]

[7] Zhao J, Wang A and Green MA. High-efficiency PERL and PERT silicon solar cells on FZ and MCZ substrates. Solar Energy Materials and Solar Cells. 2001; 65(1): 429-435. DOI: 10.1016/S0927-0248(00)00123-9 [Accessed 23th December 2021]

[8] Kluska S, Granek F. High-Efficiency Silicon Solar Cells with Boron Local Back Surface Fields Formed by Laser Chemical Processing. IEEE Electron Device Letters. 2011; 32(9): 1257-1259. DOI: 10.1109/LED.2011.2159699 [Accessed 17th December 2021]

[9] Kray D, Fell A, Hopman S, Mayer K, Willeke GP, Glunz SW. Laser Chemical Processing (LCP) - A versatile tool for microstructuring applications. Applied Physics A: Materials Science & Processing. 2008; 93: 99-103. DOI: 10.1007/s00339-008-4723-8 [Accessed 17th December 2021]

[10] Blakers AW, Wang A, Milne M, etc. 22.8% Efficient Silicon Solar Cell. Applied Physics Letters. 1989; 55(1363). Available from: https://doi.org/10.1063/1.101596 [Accessed 23th November 2021]

[11] Zhao J, Wang A, Altermatt P, Green MA. Twenty-four percent efficient silicon solar cells with double layer antireflection coatings and reduced resistance loss. Applied Physics Letters. 66, 3636 (1995). Available from: https://doi.org/10.1063/1.114124 [Accessed 15th December 2021]

[12] Zhang G, Zhao J, Green MA. Effect of substrate heating on the adhesion and humidity resistance of evaporated MgF2/ZnS antireflection coatings and on the performance of high-efficiency silicon solar cells. Solar Energy Materials and Solar Cells. 1998; 51(3-4): 393-400. Available from: https://doi.org/10.1016/S0927-0248(97)00258-4 [Accessed 15th December 2021]

[13] Kim T, Lim JK, Shin HNR, etc. 21%-efficient PERL Solar Cells with Plated Front Contacts on Industrial 156 mm p-type Crystalline Silicon Wafers. Energy Procedia. 2014; 55: 431-436. DOI: 10.1016/j.egypro.2014.08.123 [Accessed 17th December 2021]

[14] Cornagliotti E, Uruena A, Hallam B, etc. Large area p-type PERL cells featuring local p+ BSF formed by laser processing of ALD Al2O3 layers. Solar Energy Materials and Solar Cells. 2015; 138: 72-79. DOI: 10.1016/j.solmat.2015.02.034 [Accessed 17th December 2021]

[15] Tous L, Aleman M, Russell R, etc. Evaluation of advanced p-PERL and n-PERT large area silicon solar cells with 20.5% energy conversion efficiencies. Progress in Photovoltaics. 2015; 23(5): 660-670. DOI: 10.1002/pip.2478 [Accessed 20th December 2021]